Journal of Alloys and Compounds 507 (2010) 531–534

Contents lists available at ScienceDirect

Journal of Alloys and Compounds

journal homepage: www.elsevier.com/locate/jallcom

Crystallization behaviors of R_2O–Al_2O_3–SiO_2 glass–ceramics for use as anodic bonding materials

Jinshu Cheng, Dehua Xiong*, Hong Li, Hongcheng Wang

Key Laboratory of Silicate Materials Science and Engineering, Wuhan University of Technology, Ministry of Education, Wuhan 430070, China

ARTICLE INFO

Article history:
Received 7 June 2010
Received in revised form 2 August 2010
Accepted 4 August 2010
Available online 12 August 2010

Keywords:
Glass–ceramics
Li_2SiO_3
$Li_2Si_2O_5$
Anodic bonding
Coefficient of thermal expansion

ABSTRACT

In this work, the crystallization behaviors of R_2O–Al_2O_3–SiO_2 (R means K, Na and Li) glass–ceramics which was used as anodic bonding materials were discussed. The glass–ceramics with P_2O_5 as nucleation agents were investigated by means of differential scanning calorimeter (DSC), X-ray diffraction (XRD), scanning electron microscopy (SEM) and coefficient of thermal expansion (CTE) tests. The test results have shown that: the DSC trace of parent glass has two different precipitation crystallization peaks corresponding to formation the crystal phases of $Li_2Si_2O_5$ and Li_2SiO_3. According to the selected heat treatment schedules, the Li_2SiO_3 crystal phases changed into $Li_2Si_2O_5$ while the crystallization temperature at 650 °C in glass–ceramics; on the contrary, the $Li_2Si_2O_5$ crystal phases can be decomposed into Li_2SiO_3 at the crystallization temperature of 850 °C. The coefficients of thermal expansion with R_2O–Al_2O_3–SiO_2 glass–ceramics about 119–140 × 10^{-7}/°C at 450 °C, which could be nearly matched that of stainless steel (No. 430#).

1. Introduction

Glass–ceramics was found in various applications in fields of optical, electrical, biological, chemical, magnetic, microelectronics and biomedical, etc. as functional and structural materials, because of their superior thermal, mechanical, electrical and other physical properties compared to their parent glasses. Currently, Li_2O–ZnO–SiO_2 glass–ceramics have received much attentions because of wide CTE range were suitable for fabrication of hermetic seals to a variety of metals and alloys including copper, stainless steel, etc. A number of studies on crystallization behaviors and other thermo-physical properties in Li_2O–ZnO–SiO_2 glass–ceramics system have been carried out [1–5]. Anodic bonding technology was used possible to irreversibly bond different metals and semiconductors to an ion-containing glass by applying a potential between the two samples and heating them at a relatively low-temperature [6]. In recent years, Pyrex glass [7–8] and some glass–ceramics [9–14] are commonly used as bonding glass. The properties of glass-ceramics are dependant on the chemical composition and the thermal history, it is therefore important to gain a thorough understanding of the processes in the crystallization of the glass-ceramics. Shuichi Shoji [9] has made use of the existing Li_2O–Al_2O_3–SiO_2 system glass–ceramics for the silicon-based chip packaging experiments, and Yourong Huang [10] has reported that a kind of lithium aluminosilicate-β-quartz glass–ceramic contained Na_2O can be used for low-temperature bonding at 180 °C and 500 V. On the basis of our preliminary works [11–14], R_2O–Al_2O_3–SiO_2 (RAS) glass–ceramics was used as a cathode substrate material which anodic bonded to stainless steel materials. The composition and crystallization kinetic parameters of RAS parent glass were discussed by using a variety of isothermal and non-isothermal analysis techniques [11]. The influences derived from parent glass compositions and heat treatment schedules on the main crystal phases and microstructure morphology of the RAS glass–ceramics were analyzed systemically [12–14].

In the present investigation, effects of crystallization temperature on the main crystal phases, microstructure morphology and coefficient of thermal expansion (CTE) of glass–ceramics have been studied. The RAS glass–ceramics has crystal phases transfer according to the selected heat treatment schedules, the Li_2SiO_3 crystal phases had changed into $Li_2Si_2O_5$ in glass–ceramics under relatively lower crystallization temperature (about 650 °C), and the $Li_2Si_2O_5$ crystal phases can be resolved into Li_2SiO_3 in glass–ceramics at higher temperature (about 850 °C) on the contrary. The CTE of RAS glass–ceramics samples were 119–140 × 10^{-7}/°C (room temperature ~450 °C), which could be matched it of stainless steel (No. 430#) nearly.

2. Experimental procedure

2.1. Preparation of parent glass

In order to match the CTE of stainless steel (No. 430#), the RAS glass was chosen as parent glass since the coefficient of thermal expansion can be adjusted

* Corresponding author. Tel.: +86 027 87860801; fax: +86 027 87860801.
E-mail address: xiongdehua2010@gmail.com (D. Xiong).

0925-8388/$ – see front matter.
doi:10.1016/j.jallcom.2010.08.011

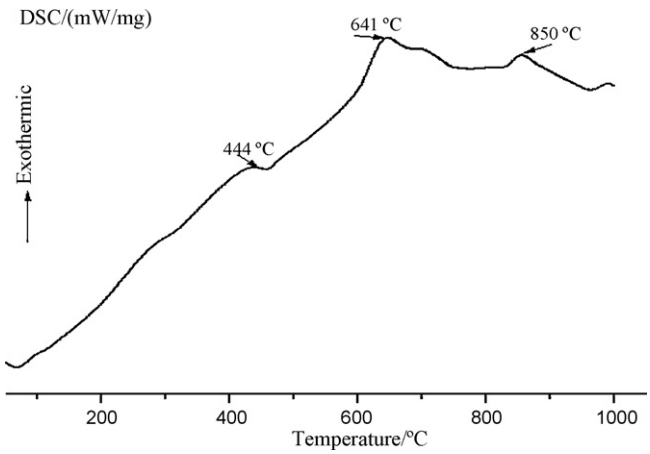

Fig. 1. DSC trace of the parent glass.

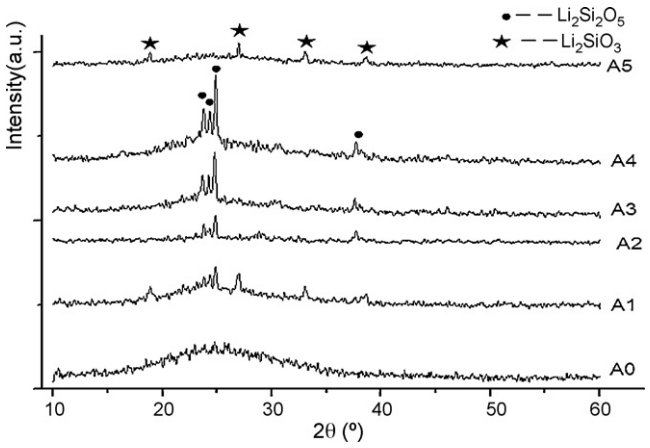

Fig. 2. The XRD patterns of samples.

within a large range by changing the heat treatment schedule. The parent glass were prepared by melting and casting, and the composition of parent glass comprised (60–68)SiO_2, (3–5)Al_2O_3, (2–3.5)ZnO, (7–10)Li_2O, (8–10)K_2O, (6–10)Na_2O, (1.5–2.5)P_2O_5 (in wt%). All raw materials were chemical reagents with pure analysis, and P_2O_5 was used as compound nucleation agent. The reagents of SiO_2, Al_2O_3, Li_2CO_3, Na_2CO_3, K_2CO_3, ZnO, and $(NH_4)H_2PO_4$ were mixed, and then they were melted in an alumina crucible at 1430–1460 °C for 3 h.The melts were casted into the pre-heated graphite mold, the parent glass was annealed at 440–480 °C for 30 min and then cooled to room temperature in the furnace naturally, and bulk transparent and parent glass without any bubbles were prepared at last.

2.2. Heat treatment schedules

The parent glass were pulverized into powder (0.150–0.075 mm) suitable for DSC employing a NETZSCH (STA 449C) DSC with the temperature range from 20 to 1000 °C. The glass powder with the weight of 30 mg was contained in a platinum crucible and the reference material was α-Al_2O_3 powders. The data were recorded by means of a chart recorder. The samples were heated in air from ambient temperature to 1000 °C at heating rates of 10 °C/min. The endothermic base line shift at 444 °C (see Fig. 1) indicates the glass transition temperature of parent glass, and the sharp exothermic peaks at the onset values of 641 and 850 °C express two crystallization temperatures for this parent glass. Combined with DSC curves and preliminary researches [11–13], the nucleate temperature of the parent glass was arranged at 500 °C and the crystallization temperature was increased from 650 to 850 °C. And kept the nucleate temperature (500 °C), nucleate time (2 h) and crystallization time (2 h) all same, the details of heat treatment schedules determined by the result of DSC curve are listed in Table 1. The parent glass was put into furnace and heated according to the scheduled temperature at 3 °C/min, and then they were kept at the setting temperatures for a period of time to nucleation and crystallization. At last, they were cooled down to room temperature naturally in the furnace.

2.3. Characterizations of glass–ceramics

1. X-ray diffraction (XRD). The glass–ceramics were pulverized into powder in agate mortar and subjected to pass 200 meshes sieve for XRD analysis. The types of crystal phases after heat treatment were analyzed by XRD (Rigaku D/Max-IIIA, Cu Kα radiation, Japan), with $2\theta = 10–60°$, working voltage 40 kV and working current 80 mA, and the diffraction patterns were analyzed by the use of MDI Jade 5.0 software.
2. Scanning electron microscope (SEM). The glass–ceramics morphology was observed by the scanning electron microscopy (JEOL, JSM-5610LV, Japan). For SEM observation, the specimen surfaces firstly were polished by diamond slurry and then etched chemically by hydrofluoric acid (5% of its volume) for 30 s at 25 °C.
3. Thermal expansion analysis. The samples were cut into strips of dimensions of 20–25mm × 4mm × 4 mm to test the coefficient of thermal expansion. The coefficients of thermal expansion of specimens were analyzed by using thermal expanding apparatus (Netzsch, DIL402C, Germany) at the heating rate of 5 °C/min.

Table 1
The heat treatment schedules of parent glass.

Sample no.	Nucleate temperature (°C)	Nucleate time (h)	Crystallization temperature (°C)	Crystallization time (h)
A0	0	0	0	0
A1	500	2	650	2
A2	500	2	700	2
A3	500	2	750	2
A4	500	2	800	2
A5	500	2	850	2

3. Results and discussion

3.1. XRD analysis

It was seen form Fig. 2, crystalline peaks corresponding to the different crystalline phases are marked with different symbols, and the crystalline phases were identified by matching the peak positions of the intense peaks with PCPDF standard cards (29-0829, 40-0376). All samples have crystal phases except parent glass (A0), Li_2SiO_3 and $Li_2Si_2O_5$ crystal phases were crystallized in glass–ceramics. The main crystal phases of A2, A3 and A4 were $Li_2Si_2O_5$, and the main crystal phases of A5 were Li_2SiO_3, but A1 has both $Li_2Si_2O_5$ and Li_2SiO_3 crystal phases. Experimental results show that all the samples have main crystal phases in a suitable heat treatment schedule, but the main crystal phases were changed with variety of crystallization temperature. From A1 to A2, relevant to the crystallization temperature increased from 650 to 700 °C, the main crystal phases have changed Li_2SiO_3 to $Li_2Si_2O_5$. On the contrary, from A4 to A5, relevant to the crystallization temperature increased from 800 to 850 °C, the main crystal phases have changed $Li_2Si_2O_5$ to Li_2SiO_3.

3.2. SEM analysis

Because all samples were chemically etched by hydrofluoric acid, and the etching rate of Li_2SiO_3 and $Li_2Si_2O_5$ are much greater than glass phase. Different from other glass–ceramics system, figure in black for the region to mean the crystallites were etched, and the light for the regional shown the residual glass phases. The crystal phases and microstructures of glass–ceramics were investigated by SEM (Fig. 3). We can see from Fig. 3, the crystal phases of A1 were needle-like Li_2SiO_3; A2, A3 and A4 were columnar $Li_2Si_2O_5$; these two crystal phases were observed in A1 but no crystal phases in A0. According to the XRD tests, there are two crystal phases in sample A1, but the amount and size of crystallites are very less, so it is not clear enough in the SEM images. With increasing the crystallization temperature, from A2 to A5, the crystal phases grow up gradually in glass–ceramics, so it is very obvious in the SEM images. Combined with the XRD tests, may be there is some chemical reaction of the phases transition between Li_2SiO_3 and $Li_2Si_2O_5$, the possible

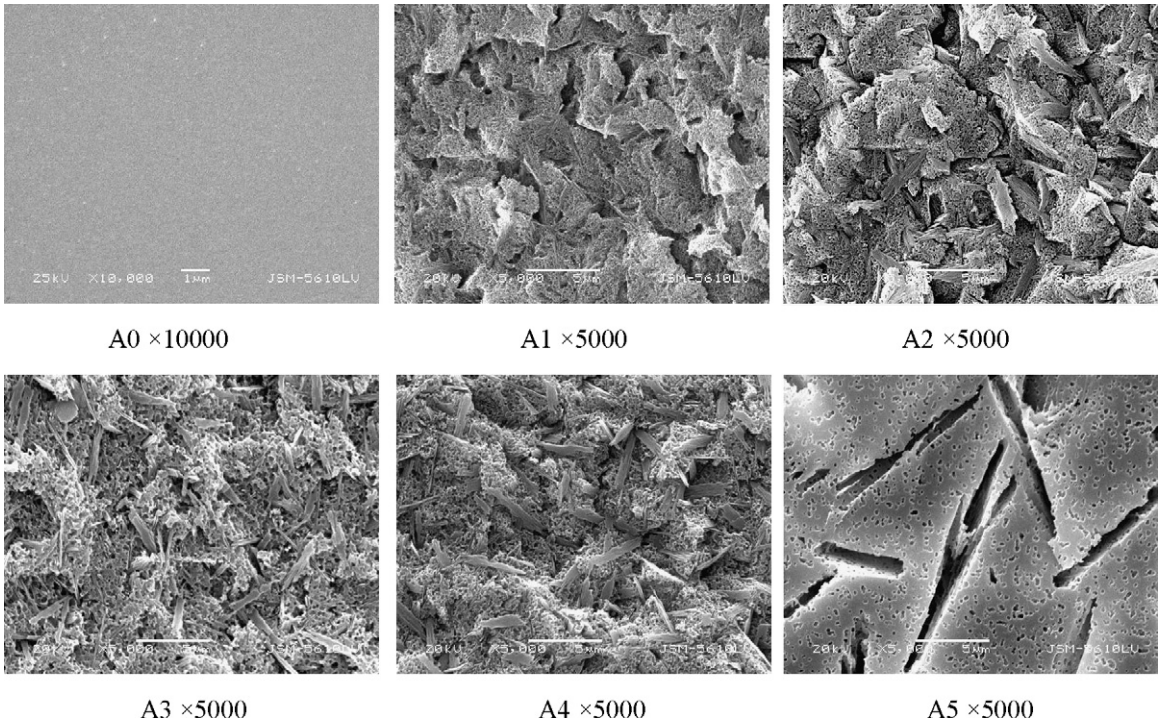

Fig. 3. SEM images of the crystal phases and microstructures of glass–ceramics.

reactions are:

$$Li_2O + SiO_2 \rightarrow Li_2SiO_3 \quad (1)$$

$$Li_2SiO_3 + SiO_2 \rightarrow Li_2Si_2O_5 \text{ (at a lower temperature)} \quad (2)$$

$$Li_2Si_2O_5 \rightarrow Li_2SiO_3 + SiO_2 \text{ (at a higher temperature)} \quad (3)$$

SEM images show that all the samples have main crystal phases with a suitable heat treatment schedules, but the amount and size of crystallites in samples do change with changing of crystallization temperature, the crystallites grew and the shape of them even more obvious when the crystallization temperature increased. All these phenomenon were similar to previous researches, Holand [15] has pointed out that lithium metasilicate and cristobalite react together to form $Li_2O{\cdot}2SiO_2$ ($Li_2Si_2O_5$) as major crystalline phase at 780 °C.

3.3. Measurement of CTE

Many factors would influence the quality of bonding, especially the linear coefficients of thermal expansion (CTE) of bonding specimens. These experiments are a kind of preparing work before the bonding of stainless steel and glass–ceramics, and the most important problem to be solved is the matching of the CTE of these two materials. The CTE of stainless steel changes with its component, while the factor of martensite and austenitic double phases stainless steel (No. 430#) were $130–150 \times 10^{-7}/°C$ (20–450 °C), and then the glass–ceramics with CTE about $130–150 \times 10^{-7}/°C$ (20–450°C) was required.

The CTE tests temperature range were 30–600 °C and the test results are listed in Table 2, the relationship of CTE between glass–ceramics are shown in Fig. 4. From Table 2, the softening point of A0 (parent glass) was 464.7 °C, the softening point of A1 and A5 were 529.4 and 531.9 °C, respectively. But the softening point of A2, A3 and A4 were greater than 600 °C, beyond the ranges of test temperature (30–600°C). RAS glass–ceramics have different softening point because of the main crystal phases in these samples have been changed. A2, A3 and A4 have the similar crystal phases ($Li_2Si_2O_5$) lead to have a minor difference on softening point. The main crystal phases in A1 and A5 were Li_2SiO_3, so the values of softening point about glass–ceramics have a major difference between A1, A5 and A2, A3, A4. All these facts were consistent to the XRD and SEM tests, and the glass–ceramics have crystal phase's change were verified again. The CTE with all samples were $119–141 \times 10^{-7}/°C$ at 450 °C, and parent glass have the biggest CTE ($140.92 \times 10^{-7}/°C$) than that of other glass–ceramics samples ($119–139 \times 10^{-7}/°C$). The thermal expansion coefficient of oxide glass is mainly determined by the bond strength between alkali metal ions and oxygen ions (anions), while the bond strength of oxygen ions proportional to the number of positive charge. The higher the valence of cations, the greater the field force of oxygen ions and alkali metal ions, thus the bond strength is greater and the thermal expansion coefficient of oxide glass is bigger. After heat treatment, the RAS glass–ceramics have main crystal with Li_2SiO_3 and $Li_2Si_2O_5$ and more Li^+ has been incorporated into the crystal, the amount of alkali metal ions was reduced and the structure of glass–ceramics becomes compact, which leads to

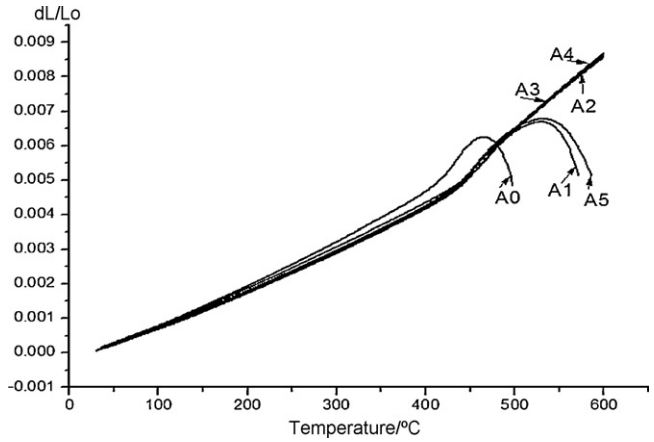

Fig. 4. The relationship of CTE between all samples.

Table 2
The results of thermal expansion coefficient tests.

Sample no.	Crystallization temperature (°C)	Crystallization time (h)	Softening point (°C)	CTE under 450 °C ($\times 10^{-7}$)
A0	0	0	464.7 ± 2	140.92
A1	650	2	529.4 ± 2	139.65
A2	700	2	>600 ± 2	122.08
A3	750	2	>600 ± 2	125.09
A4	800	2	>600 ± 2	119.84
A5	850	2	531.9 ± 2	123.45

glass–ceramics has a lower thermal expansion coefficient than parent glass.

Fig. 4 shows the relationship of CTE between all samples, glass–ceramics (A1–A5) have a smaller CTE than that of parent glass (A0) may be due to the crystal phases in them. According to the selected heat treatment schedules, the CTE with glass–ceramics were 119–140 $\times 10^{-7}$/°C at 450 °C, which could not be matched that of stainless steel (No. 430#) perfectly. So the further works would focus on changing the parent glass compositions to increase the CTE for matching that of stainless steel (No. 430#), immediately.

4. Conclusions

R_2O–Al_2O_3–SiO_2 glass–ceramics, instead of traditional hot-resistant glass was used as anodic bonding materials. Experimental results show that the crystallization temperature has great influence on the main crystal phases of this kind glass–ceramics. The main crystal phases of A2, A3 and A4 were $Li_2Si_2O_5$, and A5 was Li_2SiO_3, but A1 has these two crystal phases and A0 has not formed main crystal phases. The Li_2SiO_3 crystal phase have changed into $Li_2Si_2O_5$ when the crystallization temperature at 650 °C and $Li_2Si_2O_5$ crystal phases could be decomposed into Li_2SiO_3 while the crystallization temperature at 850 °C in this R_2O–Al_2O_3–SiO_2 glass–ceramics. After heat treatment, glass–ceramics samples have a smaller coefficients of thermal expansion than that of parent glass, the CTE of glass–ceramics were 119–140 $\times 10^{-7}$/°C at 450 °C, which could be nearly matched that of stainless steel (No. 430#).

Acknowledgements

The project was supported by the National Natural Science Foundation of China (No. 50472039) and Hubei Provincial Natural Science Foundation (No. 2005ABA011).

References

[1] Z.X. Chen, P.W. McMillan, J. Am. Ceram. Soc. 4 (1985) 220–224.
[2] S. Cramer von Clausbruch, M. Schweiger, et al., J. Non-Cryst. Solids 263–264 (2000) 388–394.
[3] B.I. Sharma, M. Goswami, et al., Mater. Lett. 58 (2004) 2423–2438.
[4] I.W. Donald, J. Non-Cryst. Solids 345–346 (2004) 120–126.
[5] M. Goswami, P. Sengupta, et al., Ceram. Int. 33 (2007) 863–867.
[6] G. Wallis, D.I. Pomerantz, J. Appl. Phys. 40 (1969) 3946–3949.
[7] A. Polyakov, P.M. Mendes, et al., 53th Electronic Components and Technology Conference, 2003, pp. 875–880.
[8] Y.-Q. Hu, Y.P. Zhao, T. Yu, Microelectron. Reliab. 48 (2008) 1720–1723.
[9] S. Shoji, H. Kikuchi, H. Torigoe, Sens. Actuators A 64 (1998) 95–100.
[10] Y. Huang, Z. Cui, X. Gao, C. Li, Z. Gu, J. Non-Cryst. Solids 354 (2008) 1407–1410.
[11] H. Li, J. Cheng, X. Cao, T. Wang, Key Eng. Mater. 336–338 (2007) 1862–1864.
[12] D. Xiong, J. Cheng, H. Li, J. Alloys Compd. 498 (2010) 162–167.
[13] D. Xiong, H. Li, J. Cheng, J. Mater. Sci.: Mater. Electron. 21 (2010) 882–888.
[14] D. Xiong, J. Cheng, H. Li, W. Deng, K. Ye, Microelectron. Eng. 87 (2010) 1741–1746.
[15] W. Holand, G. Beall, Glass Ceramic Technology, Westerville, 2000.